



Finite Element Analysis of a Novel Anatomical Locking Guide Plate for Anterior Column and Posterior Hemi-Transverse Acetabular Fractures

Junhao Deng^{1,2,3} · Ming Li^{2,3} · Jiantao Li^{2,3} · Zhirui Li^{2,3} · Fanqi Meng^{4,5} · Yanmei Zhou⁶ · Peifu Tang^{2,3} · Yanpeng Zhao^{2,3} · Licheng Zhang^{2,3}

Received: 27 April 2021 / Accepted: 31 August 2021 / Published online: 9 September 2021

© The Author(s) 2021

Abstract

Purpose The increasing worldwide prevalence of anterior column-posterior hemi-transverse fracture (ACPHTF) brings formidable challenges to orthopaedic surgeons. Our newly-designed locking plate had previously demonstrated promising effects in ACPHTF, but evidence of their direct comparison with conventional internal fixations remains lacking. In this study, we aimed to compare our novel plate with the traditional devices via finite element analysis.

Methods The ACPHTF model was created based on a 48-year-old volunteer's CT data, and then fixed in three different internal fixations: an anterior column locking plate with posterior column screws, double column locking plates, and our novel anatomical locking plate. These models were next loaded with a downward vertical force of 200 N, 400 N and 600 N, and the stress peaks and displacements of three different sites were recorded and analyzed.

Results We first tested the rigidity and found that our newly-designed locking plate as well as its matched screws had a greater stiffness especially when they were under a higher loading force of 600 N. Then we evaluated the displacements of fracture ends after applying these fixations. Both our novel plate and DLP showed significantly smaller displacement than LPPCS at the anterior column fracture line and the pubic branch fracture line, while our novel plate was not obviously inferior to DLP in terms of the displacement.

Conclusion This novel plate demonstrates a distinct superiority in the stiffness over LPPCS and DLP and comparable displacements to DLP in ACPHTF, which suggests this novel anatomical locking guide plate should be taken into consideration in ACPHTF.

Keywords Finite element analysis · Novel anatomical locking guide plate · Anterior column and posterior hemi-transverse acetabular fractures

1 Introduction

The anterior column-posterior hemi-transverse fracture (ACPHTF) is one of the most complex acetabular injuries in which treatment has, for many years, been a medical challenge to orthopaedists because of its involved location and

frequently concomitant injuries [1–3]. As a classic acetabular fracture in the elderly, ACPHTF has an increasingly high incidence with the ageing population, and is more vulnerable to acetabular protrusion and quadrilateral plate displacement [3, 4].

Therefore, an absolute anatomic reduction is indispensable as ACPHTF, usually an intra-articular fracture, is likely to cause traumatic osteoarthritis after injury [5, 6]. However, characterized by osteopenic acetabular fracture commonly seen in the geriatric population, ACPHTF is still lacking a form of adequate fracture fixation [7, 8]. Currently, the commonly reported treatment for ACPHTF was an anterior column conventional locking plate combined with posterior column screws through the ilioinguinal approach [9], or double column locking plates through

Junhao Deng and Ming Li should be considered co-first authors as they contributed equally to this paper.

✉ Yanpeng Zhao
zhaoyanpeng@plagh.org

✉ Licheng Zhang
zhanglicheng@301hospital.com.cn

Extended author information available on the last page of the article

both approach [2, 10]. However, these methods are often more invasive and require greater exposure to get better visualization, which could inevitably result in large soft tissue injuries.

We have previously established a systematic database of acetabular morphology based on the Chinese anatomical characteristics. And on this basis, we, for the first time, designed and created a novel anatomical locking guide plate (NALGP) with screw hole threads, which were conducive to stable screw fixations in the ideal acetabular sites and provided a strong internal fixation [11, 12]. Moreover, NALGP also uses two types of screws (anterior column screws and Magic screws), which therefore provides adequate fixation of both anterior and posterior columns simultaneously. An inverted Y-shape structure was then formed by the NALGP and two screws, maximizing the reconstruction of normal acetabular anatomical structure [13, 14].

No direct comparative data on our newly-designed NALGP and conventional locking plate with screws or double locking plates (DLP) are currently available in terms of the treatment of ACPHTF. Thus, in this study, we conduct a finite element analysis on (1) the conventional locking plate with posterior column screws (LPPCS), (2) DLP, and (3) NALGP with anterior column screws and Magic screws to determine which treatment could better facilitate the anatomical reduction and strong fixation after ACPHTF.

2 Materials and Methods

2.1 Three-Dimensional Modeling of the Anterior Column-Posterior Hemi-Transverse Fracture

The Dicom data from a 48-year-old male volunteer's CT scanning were imported into the Mimics 16.0 software, and the coronal, sagittal, and transverse plane were defined, respectively. We then set the threshold at 216HU-873HU in the Mimics software, created a model mask, and reconstructed the three-dimensional model of the half pelvis (Fig. 1A). This accurate geometric model was built based on the bone contour from the CT gray scale in Mimics as previously stated [15, 16].

According to the Judet and Letournel classification for acetabular fractures [17, 18], ACPHTF model was established as previously stated [3]. Briefly, the ACPHTF's one fracture line started from the 20 mm down from anterior inferior iliac spine to the superior margin of the obturator foramen, and continued to extend to the inferior margin of the obturator foramen. And the other fracture line extended from the central point of the first fracture line to the sciatic notch's most upper point (Fig. 1B).

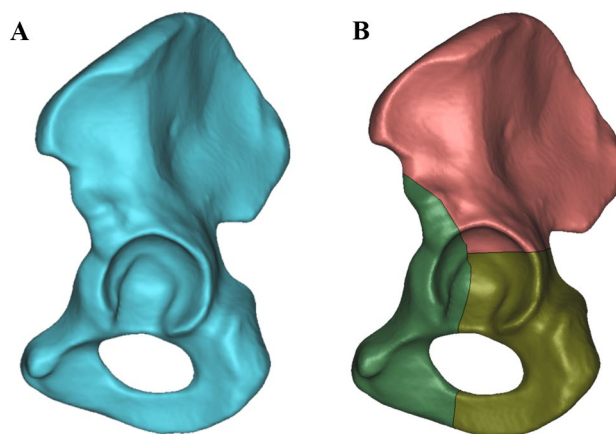


Fig. 1 The three-dimensional modeling of acetabulum and the ACPHTF. **A** Showed the normal acetabular model from the Dicom data of a 48-year-old volunteer. **B** Demonstrated the ACPHTF model and its fracture lines. Different colors were used to separate bone after ACPHTF

2.2 Geometric Modeling of Instruments Fixation in the ACPHTF

Three types of internal fixation models (including LPPCS, DLP, and NALGP) were established using the Unigraphics software (Unigraphics Solutions of EDS, USA). These models were demonstrated as follows (Fig. 2). Each assembly of the model was meshed into 8 nodes with non-linear solid hexahedron elements in the ANSYS Workbench software (ANSYS, USA). And the grid convergence were calculated by different sizes. The statistics of nodes and elements with or without instrument fixation were displayed in Table 1.

2.3 Definition of the Boundary Conditions, Material Properties, and the Loading

(1) Boundary condition

The boundary conditions were defined as follows using the Abaqus6.11 software (Dassault System, Velizy-Villacoublay, France): (1) the surface between the bone and instruments, or between instruments were both set as binding; (2) while the contact interactions between bones were assumed to be frictional [19] with a friction coefficient of 0.2.

(2) Material properties

Since materials were used to found models, we then assumed that all cortical bone, cancellous bone, and

Fig. 2 The construction of three types of internal fixation models of ACPHTF. A–C showed the LPPCS, DLP, and NALGP, respectively

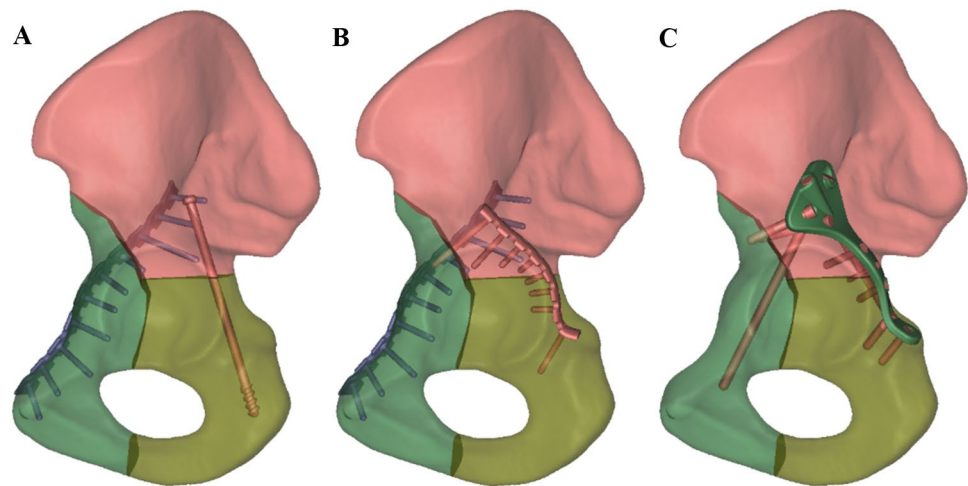


Table 1 The statistics of nodes and elements with or without instruments fixation

Model	ACPHTF		ACPHTF with fixation	
	Nodes	Elements	Nodes	Elements
LPPCS	186789	1001247	310475	206137
DLP	201465	1075243	336457	225463
NALGP	195473	1023543	314678	194587

Table 2 Bone and internal fixation material properties

Material type	Elastic modulus (MPa)	Poisson's ratio
Cortical bone	12,400	0.3
Cancellous bone	77	0.3
Instrument	110,000	0.3

internal fixations were continuous and isotropic linear elastic materials. The material properties were shown in Table 2.

(3) The applied loading and constraints

For calculation purposes, the pubic symphysis and sacroiliac joint were firmly fixed. The boundary condition of the model was set by constraining the ipsilateral ischial tuberosity and limiting its 6 degrees of freedom. As previously stated [20], in order to mimic the situation that patients with acetabular fracture were required to perform early partial weight-bearing, each assembly model was loaded with a downward vertical force of 200 N, 400 N and 600 N, respectively, at 25° backward in the sagittal plane and 45° upward in the coronal plane. The force was applied located at the middle of the hip joint.

Table 3 The von Mises stress peak of plate among three groups

Loading force model	Stress (MPa)		
	200 N	400 N	600 N
LPPCS (anterior plate)	51.547	85.422	150.174
DLP (anterior plate)	47.432	68.182	98.188
DLP (posterior plate)	21.48	86.096	147.603
NALGP (posterior plate)	44.58	97.254	191.53

2.4 Evaluation Index Among Three Types of Fixation

We first evaluated the stress distribution and stress peak of plates and screws [21], and then the displacement of fracture ends under the loading force of 200 N, 400 N and 600 N, respectively. Both stress distribution and stress peak can well reflect the rigidity of those instruments, which helps to choose suitable materials. And the displacement is a good indicator of the stability of internal fixation on the ACPHTF.

3 Results

3.1 Stress Distribution and Stress Peak

We firstly tested the rigidity of the three internal fixations and found that there were significant differences in the stress distribution of both plates and screws. Under the loading force of 200 N, 400 N, and 600 N, the von Mises stress peak of plate in the LPPCS was 51.547 MPa, 85.422 MPa, 150.174 MPa, and the Von Mises stress peak of anterior and posterior plate in the DLP were 47.432 and 21.48 MPa, 68.182 and 86.096 MPa, 98.188 and 147.603 MPa, and stress peak of novel plate in NALGP was 44.58 MPa, 97.254 MPa, 191.53 MPa (Table 3;

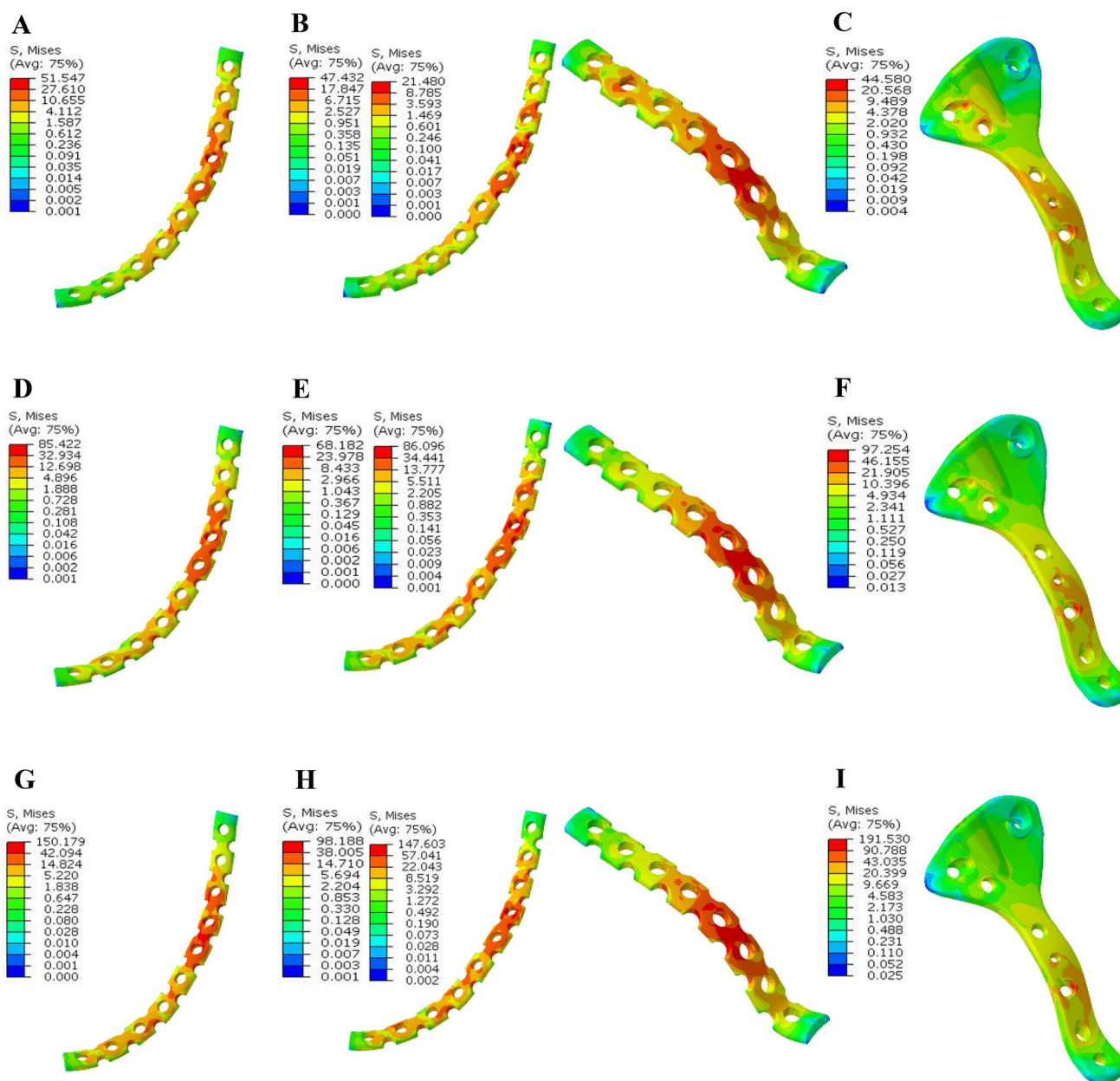


Fig. 3 The stress nephogram of plate among three groups. **A, D, and G** represent the LPPCS group, **B, E, and H** represent the DLP group, and **C, F, and I** represent the NALGP group. **A–C** were under the loading force of 200 N, **D–F** were under the loading force of 400 N,

and **G–I** were under the loading force of 600 N. The left of **B, E, and H** showed the anterior column plate, while the right showed the posterior column plate. The red areas in the plate withstood the maximum force, whereas the blue area experienced the minimum force

Fig. 3). As for the screws under the same loading force, the stress peak of anterior and posterior screws in the LPPCS were 47.941 and 22.123 MPa, 82.496 and 66.812 MPa, 142.951 and 125.812 MPa, and in the DLP were 47.302 and 88.909 MPa, 74.767 and 129.725 MPa, 120.207 and 155.777 MPa, and in the NALGP was 59.047 MPa, 105.793 MPa, and 195.066 MPa, respectively (Table 4; Fig. 4).

Table 4 The Von Mises stress peak of screws among three groups

Loading force model	Stress (MPa)		
	200 N	400 N	600 N
LPPCS (anterior screw)	47.941	82.496	142.951
LPPCS (posterior screw)	22.123	66.812	125.812
DLP (anterior screw)	47.302	74.767	120.207
DLP (posterior screw)	88.909	129.725	155.777
NALGP (posterior screw)	59.047	105.793	195.066

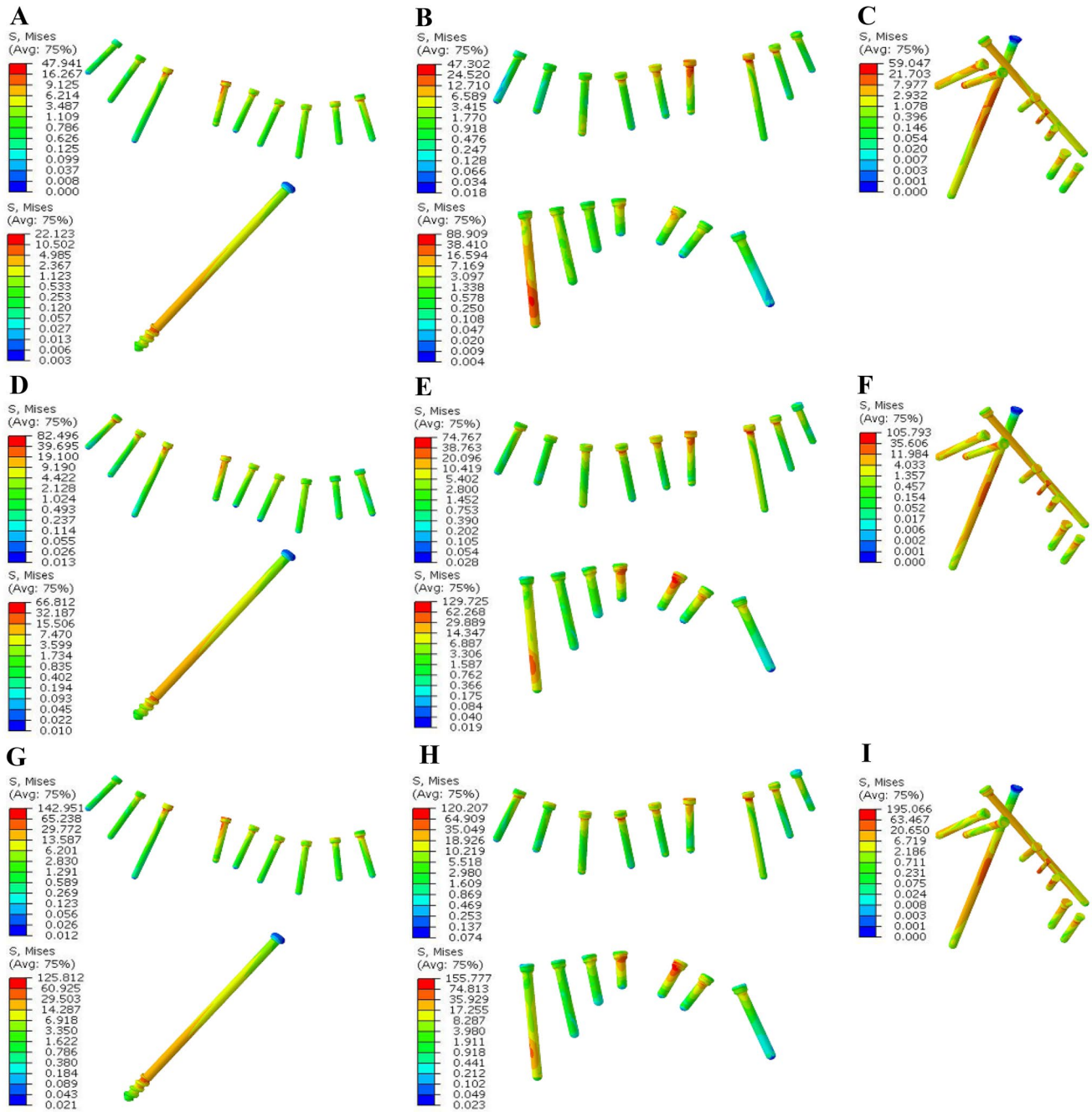


Fig. 4 The stress nephogram of screws among three groups. **A, D,** and **G** represent the LPPCS group, **B, E,** and **H** represent the DLP group, and **C, D,** and **I** represent the NALGP group. **A–C** were under the loading force of 200 N, **D–F** were under the loading force of 400 N, and **G–I** were under the loading force of 600 N. The top of **A,**

B, D, E, G and **H** showed the anterior column screws, while the bottom showed the posterior column screws. The red areas in the screw withstood the maximum force, whereas the blue area experienced the minimum force

3.2 Displacement

We next evaluated the maximum displacement of the fracture at the three sites: the transverse fracture line (TF), anterior column fracture line (ACF), and the pubic branch fracture line (PBF).

At the site of TF line and under the loading force of 200 N, 400 N, and 600 N, the maximum displacement in the LPPCS was 0.089 mm, 0.101 mm, and 0.126 mm, and in the DLP was 0.057 mm, 0.071 mm, and 0.112 mm, and in the NALGP was 0.062 mm, 0.082 mm, and 0.124 mm, respectively. At the site of ACF and under the same loading force,

the maximum displacement in the LPPCS was 0.032 mm, 0.035 mm, and 0.041 mm, and in the NALGP was 0.038 mm, 0.042 mm, and 0.077 mm, respectively. Similarly, the maximum displacement at the PBF in the LPPCS was 0.124 mm, 0.191 mm, and 0.273 mm, and in the DLP was 0.094 mm, 0.12 mm, and 0.183 mm, and in the NALGP was 0.107 mm, 0.132 mm, and 0.191 mm, respectively (Table 5; Fig. 5).

4 Discussion

In this study, we performed a finite element analysis of a NALGP with an anterior column screw and magic screw for anterior column and posterior hemi-transverse acetabular fractures. Two main results have been found: (1) compared with other two groups, our newly-designed anatomical locking guide plate as well as its matched screws had a greater rigidity especially when they were under a higher loading force of 600 N; (2) compared with the LPPCS, both our novel plate and DLP provided a better stability in the treatment of ACPHTF. And the novel plate was comparable to DLP with regards to the maximum displacement as a whole.

In fact, ACPHTF has an increasing prevalence in the growing elderly population in recent years. This classic osteopenic acetabular fracture generally requires early anatomical reduction and rigid internal fixation post injury [8, 22, 23]. However, it remains controversial on which internal fixation should be taken for the treatment of this type of acetabular fracture. Previously, our newly-designed anatomical locking plate was reported to have a promising effect on the acetabular fracture with a small sample [12], but no direct comparison between our novel plate and traditional internal fixation on the ACPHTF has been conducted to date. Therefore, we conducted this study using finite element analysis.

To simulate the partial or full weight-bearing loading after ACPHTF, partial loading force of 200 N and 400 N, and full loading force of 600 N were set in this study. First, we compared the stress distribution between this novel plate with its screws and those conventional plates and screws. Stress distribution could imply the ability of plates or screws to resist the elastic deformation when subjected to force, as stress concentration is likely to cause plate or

screw deformation or even breakage [24]. Whether it be under the force of 200 N, 400 N or 600 N, from the stress nephogram we could easily tell that the stress distribution of plate and screws in the NALGP group were more uniform and less concentrated, although there was higher stress on the plates and screws in the NALGP group compared with those in other groups.

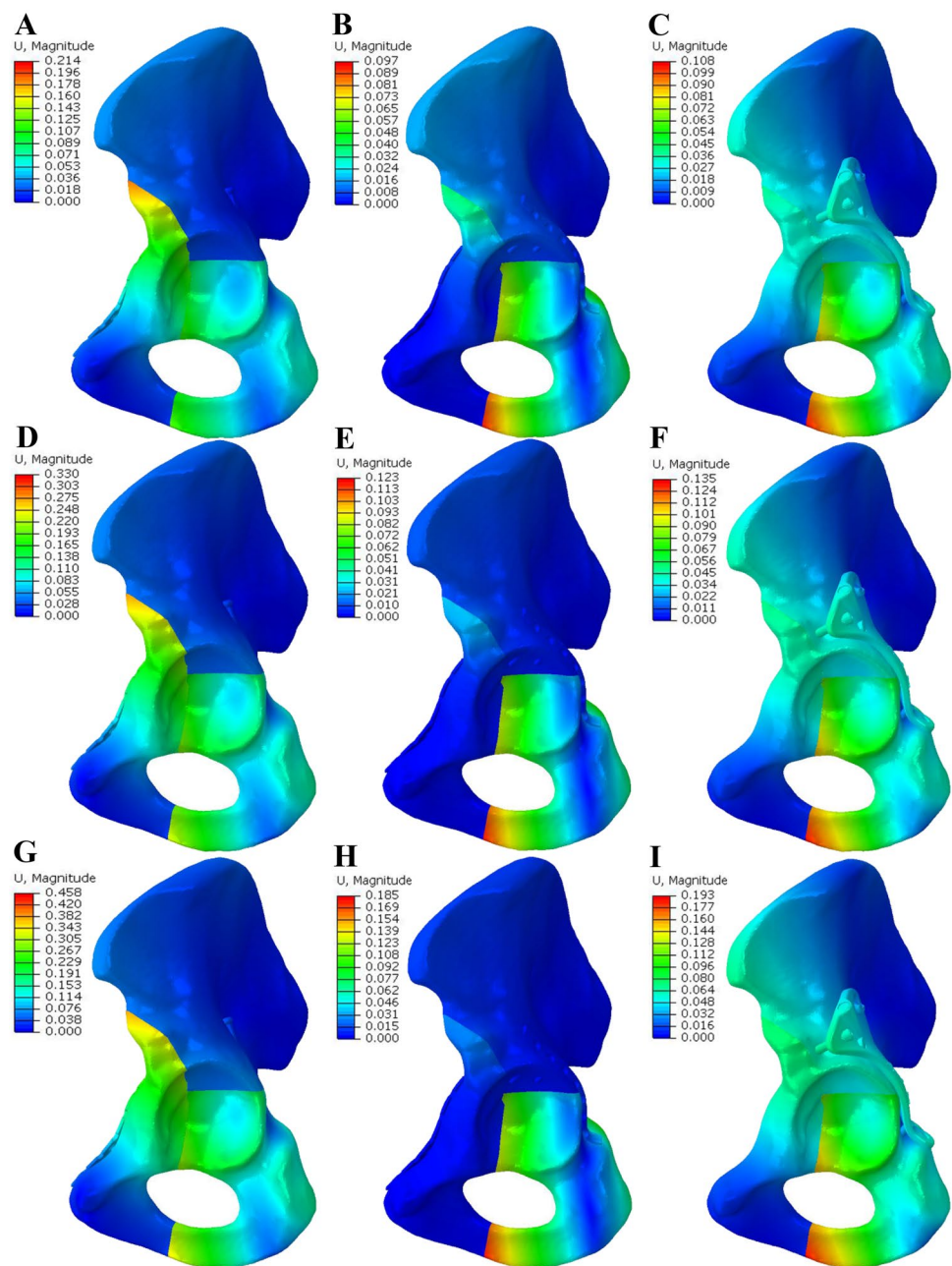
Then, we observed the maximum displacement at three different sites after the weight-bearing loading. The LPPCS showed the much greater displacement when compared with other two groups, whether it be the fracture site or the size of loading force, although comparatively, LPPCS showed a little better stability at the TF site within group comparison. The DLP group unsurprisingly demonstrated the optimal stability in the treatment of ACPHTF, regardless of the site or loading force. However, DLP demands bigger surgical exposure, and longer operative time, which would therefore induce greater soft tissue injury and other concomitant risks [25]. On the other hand, compared with the DLP group, the NALGP group displayed a comparable displacement almost in all three sites and types of loading force, but experienced a slightly higher shift at the site of ACF. Namely, NALGP might not be as good as DLP in terms of anterior column stability with a loading force of 600 N.

NALGP, an inverted Y-shape structure plate, was designed on the basis of the acetabulum morphology of Chinese patients, which therefore could match the acetabular structure very well. Unlike the previous plates, there is no need to pre-contour our newly-designed plate, minimizing the operative time [12]. Notably, the NALGP has a fan-shape structure in the rostral part, offering more stable fixation to the top of acetabular and then going a long way towards the treatment of acetabular fracture with top comminution. Moreover, the guiding screw hole embedded in the NALGP tells the surgeon where to put their screws, making possible the minimally invasive screw implants. After this finite element analysis of NALGP, we further confirmed its advantages in rigidity and stability. Thus, taking the superiorities of NALGP into consideration, we would recommend the NALGP as the first choice for ACPHTF especially the patients with better stability of anterior column in this study.

Table 5 The maximum displacement of fracture at three sites among three groups

Site	The maximum displacement (mm)								
	TF			ACF			PBF		
Force	200 N	400 N	600 N	200 N	400 N	600 N	200 N	400 N	600 N
Model									
LPPCS	0.089	0.101	0.126	0.168	0.215	0.321	0.124	0.191	0.273
DLP	0.057	0.071	0.112	0.032	0.035	0.041	0.094	0.12	0.183
NALGP	0.062	0.082	0.124	0.038	0.042	0.077	0.107	0.132	0.191

Fig. 5 The maximum displacement of fractures at three sites. **A, D, and G** represent the LPPCS group, **B, E, and H** represent the DLP group, and **C, F, and I** represent the NALGP group. **A–C** were under the loading force of 200 N, **D–F** were under the loading force of 400 N, and **G–I** were under the loading force of 600 N. The red areas in the hip experienced the maximum deformation, whereas the blue area experienced the minimum deformation



As comparison results of this study were dependent on the accuracy of the FE model [2], it's necessary to make clear the accuracy of our FE model. Indeed, our FE model building procedures and parameters applied were strictly abided by previous studies [15, 16], in which they employed similar loading and boundary conditions. Moreover, the aim of this study was to test trends rather than absolute values among three groups. Taking that into consideration, we suppose that this research may be reasonable and reliable.

This finite element analysis study also has some limitations. First, we applied to the computer programs instead of the real environment, which inevitably lost some unknown

information. We would next perform a cohort study to further explore the advantages and disadvantages of our novel plates. Second, we only compared the NAGLP with two classic internal fixations. But as a controversial medical challenge, ACPHTF also had other types of fixation. More comparisons were needed in the next study.

5 Conclusion

Taken together, the major findings of our study were 1. compared with the LPPCS and DLP group, our newly-designed anatomical locking guide plate as well as its matched screws had a greater rigidity especially when they were under a higher loading force of 600 N; 2. compared with the LPPCS, both our novel plate and DLP provided a better stability in the treatment of ACPHTF. And the novel plate was comparable to DLP with regards to the maximum displacement as a whole. This NALGP with an anterior column screw and magic screw should be taken into consideration in the treatment of ACPHTF.

Open Access This article is licensed under a Creative Commons Attribution 4.0 International License, which permits use, sharing, adaptation, distribution and reproduction in any medium or format, as long as you give appropriate credit to the original author(s) and the source, provide a link to the Creative Commons licence, and indicate if changes were made. The images or other third party material in this article are included in the article's Creative Commons licence, unless indicated otherwise in a credit line to the material. If material is not included in the article's Creative Commons licence and your intended use is not permitted by statutory regulation or exceeds the permitted use, you will need to obtain permission directly from the copyright holder. To view a copy of this licence, visit <http://creativecommons.org/licenses/by/4.0/>.

References

- Chen, K., Yang, F., Yao, S., Xiong, Z., Sun, T., et al. (2020). Biomechanical comparison of different fixation techniques for typical acetabular fractures in the elderly: The role of special quadrilateral surface buttress plates. *Journal of Bone and Joint Surgery. American Volume*, *102*(14), e81.
- Lei, J., Dong, P., Li, Z., Zhu, F., Wang, Z., et al. (2017). Biomechanical analysis of the fixation systems for anterior column and posterior hemi-transverse acetabular fractures. *Acta Orthopaedica et Traumatologica Turcica*, *51*(3), 248–253.
- Tanoglu, O., Alemdaroglu, K. B., Iltar, S., Ozmeric, A., Demir, T., et al. (2018). Biomechanical comparison of three different fixation techniques for anterior column posterior hemitransverse acetabular fractures using anterior intrapelvic approach. *Injury*, *49*(8), 1513–1519.
- May, C., Egloff, M., Butscher, A., Keel, M. J. B., Aebi, T., et al. (2018). Comparison of fixation techniques for acetabular fractures involving the anterior column with disruption of the quadrilateral plate: A biomechanical study. *Journal of Bone and Joint Surgery*, *100*(12), 1047–1054.
- Gillispie, G. J., Babcock, S. N., McNamara, K. P., Dimoff, M. E., Aneja, A., et al. (2017). Biomechanical comparison of intrapelvic and extrapelvic fixation for acetabular fractures involving the quadrilateral plate. *Journal of Orthopaedic Trauma*, *31*(11), 570–576.
- Gras, F., Marintschev, I., Schwarz, C. E., Hofmann, G. O., Pohlemann, T., et al. (2012). Screw- versus plate-fixation strength of acetabular anterior column fractures: A biomechanical study. *Journal of Trauma and Acute Care Surgery*, *72*(6), 1664–1670.
- Spitler, C. A., Kiner, D., Swafford, R., Doty, D., Goulet, R., et al. (2017). Generating stability in elderly acetabular fractures—A biomechanical assessment. *Injury*, *48*(10), 2054–2059.
- Butterwick, D., Papp, S., Gofton, W., Liew, A., & Beaulé, P. E. (2015). Acetabular fractures in the elderly: Evaluation and management. *Journal of Bone and Joint Surgery. American Volume*, *97*(9), 758–768.
- Letournel, E. (1993). The treatment of acetabular fractures through the ilioinguinal approach. *Clinical Orthopaedics and Related Research*, *292*, 62–76.
- Yildirim, A. O., Alemdaroglu, K. B., Yuksel, H. Y., Oken, O. F., & Ucaner, A. (2015). Finite element analysis of the stability of transverse acetabular fractures in standing and sitting positions by different fixation options. *Injury*, *46*(Suppl 2), S29–S35.
- Xu, M., Zhang, L. H., Zhang, Y. Z., He, C. Q., Zhang, L. C., et al. (2013). Development of site-specific locking plates for acetabular fractures. *Orthopedics*, *36*(5), e593–e600.
- Xu, M., Zhang, L. H., Zhang, Y. Z., Zhang, L. C., He, C. Q., et al. (2014). Custom-made locked plating for acetabular fracture: A pilot study in 24 consecutive cases. *Orthopedics*, *37*(7), e660–e670.
- Zhang, L., Zhang, W., Mullis, B., Liu, D., Xiong, Q., et al. (2016). Percutaneous anterior column fixation for acetabulum fractures, does it have to be difficult?—The new axial pedicle view of the anterior column for percutaneous fixation. *Journal of Orthopaedic Trauma*, *30*(1), e30–e35.
- Zhang, L. H., Zhang, L. C., Si, Q. H., Gao, Y., Su, X. Y., et al. (2016). Experimental study on treatment of acetabular anterior column fractures: Application of a minimally invasive percutaneous lag screw guide apparatus. *BMC Musculoskeletal Disorders*, *17*, 27.
- Anderson, A. E., Peters, C. L., Tuttle, B. D., & Weiss, J. A. (2005). Subject-specific finite element model of the pelvis: Development, validation and sensitivity studies. *Journal of Biomechanical Engineering*, *127*(3), 364–373.
- Dalstra, M., & Huiskes, R. (1995). Load transfer across the pelvic bone. *Journal of Biomechanics*, *28*(6), 715–724.
- Letournel, E. (2019). Acetabulum fractures: Classification and management. *Journal of Orthopaedic Trauma*, *33*(Suppl 2), S1–S2.
- Beaulé, P. E., Dorey, F. J., & Matta, J. M. (2003). Letournel classification for acetabular fractures. Assessment of interobserver and intraobserver reliability. *The Journal of Bone and Joint Surgery*, *85*(9), 1704–1709.
- Ezquerria, L., Quilez, M. P., Perez, M. A., Albareda, J., & Seral, B. (2017). Range of movement for impingement and dislocation avoidance in total hip replacement predicted by finite element model. *Journal of Medical and Biological Engineering*, *37*(1), 26–34.
- Khajavi, K., Lee, A. T., Lindsey, D. P., Leucht, P., Bellino, M. J., et al. (2010). Single column locking plate fixation is inadequate in two column acetabular fractures. A biomechanical analysis. *Journal of Orthopaedic Surgery and Research*, *5*, 30.
- Samsami, S., Saberi, S., Sadighi, S., & Rouhi, G. (2015). Comparison of three fixation methods for femoral neck fracture in young adults: Experimental and numerical investigations. *Journal of Medical and Biological Engineering*, *35*(5), 566–579.
- Culemann, U., Holstein, J. H., Kohler, D., Tzioupis, C. C., Pizanis, A., et al. (2010). Different stabilisation techniques for typical acetabular fractures in the elderly—A biomechanical assessment. *Injury*, *41*(4), 405–410.
- Briffa, N., Pearce, R., Hill, A. M., & Bircher, M. (2011). Outcomes of acetabular fracture fixation with ten years' follow-up. *Journal of Bone and Joint Surgery. British Volume*, *93*(2), 229–236.
- Zhang, D., Liu, N., Chen, Y., Zhang, G., Tian, J., et al. (2020). Microstructure evolution and mechanical properties of PM-Ti₄₃Al₉V_{0.3}Y Alloy. *Materials (Basel)*, *13*(1), 198–207.

25. Giordano, V., de Amaral, N. P., Pallottino, A., Pires e Albuquerque, R., Franklin, C. E., et al. (2009). Operative treatment of transverse acetabular fractures: Is it really necessary to fix both columns? *International Journal of Medical Sciences*, 6(4), 192–199.

Authors and Affiliations

Junhao Deng^{1,2,3} · Ming Li^{2,3} · Jiantao Li^{2,3} · Zhirui Li^{2,3} · Fanqi Meng^{4,5} · Yanmei Zhou⁶ · Peifu Tang^{2,3} · Yanpeng Zhao^{2,3} · Licheng Zhang^{2,3}

Junhao Deng
deng_junh@163.com

Ming Li
liming891215@163.com

Jiantao Li
lijiantao618@163.com

Zhirui Li
lizhirui@301hospital.com.cn

Fanqi Meng
fanqimeng@pku.edu.cn

Yanmei Zhou
zhouym@szbl.ac.cn

Peifu Tang
pftang301@163.com

² Department of Orthopaedics, Chinese PLA General Hospital, No. 28 Fuxin Road, Beijing 100853, People's Republic of China

³ National Clinical Research Center for Orthopedics, Sports Medicine & Rehabilitation, No. 28 Fuxin Road, Beijing 100853, People's Republic of China

⁴ Department of Spine Surgery, Peking University People's Hospital, Beijing 100044, People's Republic of China

⁵ Institute of Orthopaedics, Chinese PLA General Hospital, No. 28 Fuxin Road, Beijing 100853, People's Republic of China

⁶ Shenzhen Bay Laboratory, No. 2199 Lishui Road, Shenzhen 518132, Guangdong Province, People's Republic of China

¹ Medical School of Chinese PLA, No. 28 Fuxin Road, Beijing 100853, People's Republic of China